

Numerical simulation of an inviscid transonic flow through a channel with a leap

P. LISEWSKI (WARSZAWA)

A TWO-DIMENSIONAL inviscid transonic channel flow of a perfect gas is considered. The gas of relatively high pressure, flows into a channel through a converging nozzle. The channel geometry is characterised by a discontinuity of cross-section at the nozzle outlet. A fast, explicit differential algorithm based on a two-step Lax–Wendroff scheme is used to solve the set of Euler equations. Results of calculations are compared with the visualised flow and with the measured pressure distributions. The computed steady-state flow field agrees well with measurements.

Notations

- a speed of sound,
- e total energy per unit mass,
- \mathbf{F}, \mathbf{G} flux vectors,
- H channel height,
- J Jacobian determinant,
- k specific heats ratio,
- L channel length,
- p_0 stagnation pressure at the nozzle inlet,
- p_{out} pressure in a large volume at the outlet of the channel,
- $R+$ right running Riemann invariant,
- $R-$ left running Riemann invariant,
- t time,
- u velocity component in x direction,
- v velocity component in y direction,
- T_0 stagnation temperature at the nozzle inlet,
- \mathbf{U} flow variable vector,
- x, y coordinates in physical plane,
- Δl distance between two nodes in physical plane,
- Δt time step,
- $\Delta \eta$ distance between two nodes in η direction,
- $\Delta \xi$ distance between two nodes in ξ direction,
- ξ, η coordinates in computational plane,
- ρ density,
- φ ratio of the nozzle exit height to channel height.

1. Introduction

TRANSONIC FLOWS through channels with abrupt changes of cross-section can be found in practice in reducing valves or industrial installations. The structure of the flow field depends on the geometry of the channel and on the difference of pressures in the areas situated at the channel inlet and outlet. If the cross-section of the channel changes sharply and the pressure difference is high enough, shock waves may occur in the flow. Determining such flows field seems to be important from practical point of view.

Contemporary techniques of solving transonic flow problems can be grouped generally in two categories. The first contains methods that use central difference approximation applied to spatial derivatives. One can find here both explicit and implicit algorithms of different order of accuracy in time and space. Lax–Wendroff and Beam–Warming approaches are the most popular in this group. The second family of numerical methods for transonic aerodynamics contains the so-called “upwind” schemes. Their nature is closer to physics as they distinguish directions of the propagation of information in the flow. Different approaches of Godunov-type methods can be found in this category.

In the present work, a central difference method based on two-step Lax–Wendroff scheme has been chosen to solve two-dimensional inviscid transonic flow. This method is believed to be simpler to implement as compared with upwind schemes. It requires less arithmetic operations per time step than the explicit upwind algorithms. Hence, it is less time-consuming.

2. Problem description

A two-dimensional, inviscid flow of continuous medium is assumed. The gas flows through a two-dimensional (plane) channel shown schematically in Fig. 1. The first part of the channel consists of a converging nozzle and the second part is a duct of constant cross-section. Air flows into the channel from a large volume characterised by constant stagnation pressure (p_0) and temperature (T_0). At the channel outlet air flows into the surroundings where constant pressure (p_{out}) is assumed. The flow starts after breaking a diaphragm placed at the nozzle inlet.

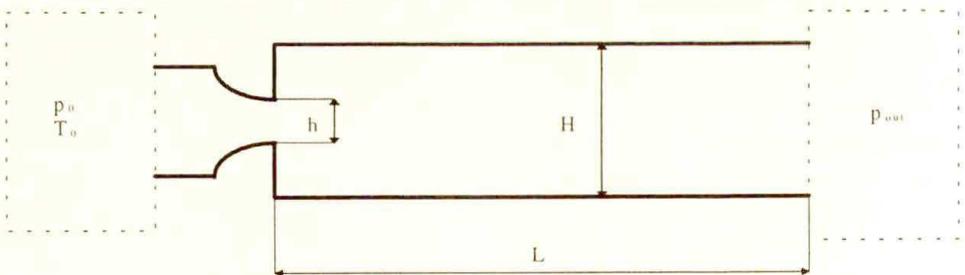


FIG. 1. Shape of the channel.

Air is treated as a perfect gas. A limiting case of steady-state solution is of interest.

3. Mathematical formulation

The inviscid unsteady two-dimensional flow without body forces and heat transfer is described in differential conservative form by Euler equations, i.e. the continuity, momentum and energy equations. This set of equations can be written in a vector form:

$$(3.1) \quad \frac{\partial \mathbf{U}}{\partial t} + \frac{\partial \mathbf{F}}{\partial x} + \frac{\partial \mathbf{G}}{\partial y} = 0.$$

The vectors are:

$$(3.2) \quad \mathbf{U} = \begin{Bmatrix} \rho \\ \rho u \\ \rho v \\ \rho e \end{Bmatrix}, \quad \mathbf{F} = \begin{Bmatrix} \rho u \\ \rho u^2 + p \\ \rho uv \\ u(\rho e + p) \end{Bmatrix}, \quad \mathbf{G} = \begin{Bmatrix} \rho v \\ \rho uv \\ \rho v^2 + p \\ v(\rho e + p) \end{Bmatrix}.$$

The total energy per unit mass is expressed by

$$e = \frac{p}{(k - 1)\rho} + \frac{1}{2} (u^2 + v^2).$$

By knowing the initial and boundary conditions, Eq. (3.1) can be integrated to provide the inviscid solution at a later time. Since the steady flow can be considered as a special case of unsteady flow, the steady-state solution can also be obtained from unsteady Euler equations as an asymptotic case.

For flows in complex geometries it is advantageous to transform the set of Eqs. (3.1) to the generalised, curvilinear coordinate system. General relations between the coordinates in the computational plane of reference and in the physical plane of reference are:

$$(3.3) \quad \xi = \xi(x, y), \quad \eta = \eta(x, y).$$

After the transformation has been applied, Eq. (3.1) preserves its strong conservation form:

$$(3.4) \quad \frac{\partial \bar{\mathbf{U}}}{\partial t} + \frac{\partial \bar{\mathbf{F}}}{\partial \xi} + \frac{\partial \bar{\mathbf{G}}}{\partial \eta} = 0,$$

where “new” flow variable vector and “new” flux vectors are:

$$(3.5) \quad \bar{\mathbf{U}} = \frac{\mathbf{U}}{J}, \quad \bar{\mathbf{F}} = \frac{\xi_x \mathbf{F} + \xi_y \mathbf{G}}{J}, \quad \bar{\mathbf{G}} = \frac{\eta_x \mathbf{F} + \eta_y \mathbf{G}}{J}.$$

The Jacobian of the transformation is given by

$$(3.6) \quad J = \xi_x \eta_y - \xi_y \eta_x = \frac{1}{x_\xi y_\eta - x_\eta y_\xi}.$$

The metrics are:

$$(3.7) \quad \xi_x = y_\eta \cdot J, \quad \xi_y = -x_\eta \cdot J, \quad \eta_x = -y_\xi \cdot J, \quad \eta_y = x_\xi \cdot J.$$

4. Numerical method

As the aim of this work is to investigate transonic channel flow, it is necessary to use a method that captures well the shock waves occurring in the flow. As mentioned in the introduction, a modified two-step differential scheme based on Lax – Wendroff – Richtmyer formulation [1, 3] is used to solve the set of equations (3.1) in the computational plane of reference. The formulation applied in the current work is described below.

During the first step, the values at the intermediate time level are calculated:

$$(4.1) \quad \begin{aligned} \bar{\mathbf{U}}_{i+1/2,j}^{n+1/2} = & \frac{1}{4} \left(\bar{\mathbf{U}}_{i+1,j}^n + \bar{\mathbf{U}}_{i,j}^n + \bar{\mathbf{U}}_{i+1/2,j+1/2}^n + \bar{\mathbf{U}}_{i+1/2,j-1/2}^n \right) \\ & - \frac{1}{2} \frac{\Delta t}{\Delta \xi} \left(\bar{\mathbf{F}}_{i+1,j}^n - \bar{\mathbf{F}}_{i,j}^n \right) - \frac{1}{2} \frac{\Delta t}{\Delta \eta} \left(\bar{\mathbf{G}}_{i+1/2,j+1/2}^n - \bar{\mathbf{G}}_{i+1/2,j-1/2}^n \right). \end{aligned}$$

New values of the flow variable vector \mathbf{U} are obtained from the final step:

$$(4.2) \quad \bar{\mathbf{U}}_{i,j}^{n+1} = \bar{\mathbf{U}}_{i,j}^n - \frac{\Delta t}{\Delta \xi} \left(\bar{\mathbf{F}}_{i+1,j}^{n+1/2} - \bar{\mathbf{F}}_{i-1/2,j}^{n+1/2} \right) - \frac{\Delta t}{\Delta \eta} \left(\bar{\mathbf{G}}_{i,j+1/2}^{n+1/2} - \bar{\mathbf{G}}_{i,j-1/2}^{n+1/2} \right).$$

The flux vector \mathbf{F} based on middle nodes is calculated as follows (the flux vector \mathbf{G} is calculated similarly):

$$(4.3) \quad \begin{aligned} \bar{\mathbf{F}}_{i+1/2,j+1/2}^n &= \bar{\mathbf{F}} \left(\frac{\bar{\mathbf{U}}_{i+1,j}^n + \bar{\mathbf{U}}_{i+1,j+1}^n + \bar{\mathbf{U}}_{i,j+1}^n + \bar{\mathbf{U}}_{i,j}^n}{4} \right), \\ \bar{\mathbf{F}}_{i+1/2,j}^{n+1/2} &= \bar{\mathbf{F}} \left(\bar{\mathbf{U}}_{i+1/2,j}^{n+1/2} \right). \end{aligned}$$

The described algorithm differs from the Richtmyer's version [1, 3]. Its main advantage is that averaging of flow variables, necessary to calculate the flux vectors at points located between nodes (see (4.1)), takes place only on the basic time level. Values obtained from the intermediate step (4.1) having no physical meaning, serve only for further calculations.

The described integration method is of second-order accuracy in space and time. As it is an explicit method, the maximal time step is limited by the stability

criteria (CFL number). In the present work the size of time step is obtained from the condition

$$\Delta t \leq \min \left(\Delta l / \sqrt{2} \cdot \left(\sqrt{u^2 + v^2} + a \right) \right).$$

The method chosen, applied to transonic flow problems, requires artificial damping in order to minimise oscillations produced around the captured shocks. The effect of artificial viscosity has been introduced by adding the third, smoothing step in which the solution obtained from the Lax – Wendroff final step (4.2) is corrected proportionally to the second spatial derivative, separately for ξ and η directions.

5. The physical plane of reference

Because of the symmetry of the steady-state flow, the physical plane of reference can consist only of one half of a real channel. The shape of this area is shown in Fig. 2. It contains two subregions: the first one, corresponding to a converging nozzle and the second, corresponding to the part of the channel of constant cross-section. These two subregions are connected at the nozzle outlet.

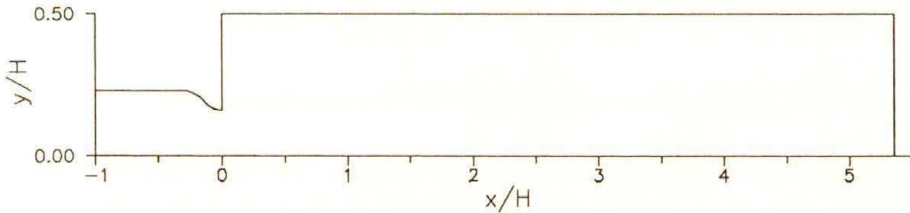


FIG. 2. Physical plane of reference.

6. Numerical implementation of boundary conditions

At the inlet boundary, a quasi-one-dimensional boundary condition is applied. Stagnation pressure p_0 and temperature T_0 are imposed. These values are assumed to be constant over the channel width at the inlet. The energy equation and the Riemann invariant $R-$ (calculated from the interior of the flow field) are used to find static parameters at the nozzle inlet. The value of $R-$ is found with the method of characteristics, assuming linear interpolation of flow variables between nodes.

At the outlet boundary similar treatment is made. Subsonic and supersonic cases are considered separately. At the subsonic outlet, the only variable to be imposed is static pressure.

In the supersonic outflow, no information from outside is coming upstream. In this case both Riemann invariants along suitable characteristics, combined with

the value of entropy along the streamline, are used to calculate flow variables at the channel outlet.

Rigid walls are modelled by superimposing the layer of fictitious nodes placed behind the walls.

At the near axis boundary the symmetry condition is applied.

At the nozzle exit, the exchange of information between two computational subdomains is assured.

7. Sample calculation of the flow field

The calculated steady-state flow field in the wide part of the channel is shown in Fig. 3. The gas flows from the left to the right. The figure presents pressure contours obtained for $\varphi = 0.3$ $L/H = 5.33$ ($L = 160$ mm) and $p_{\text{out}}/p_0 = 0.132$.

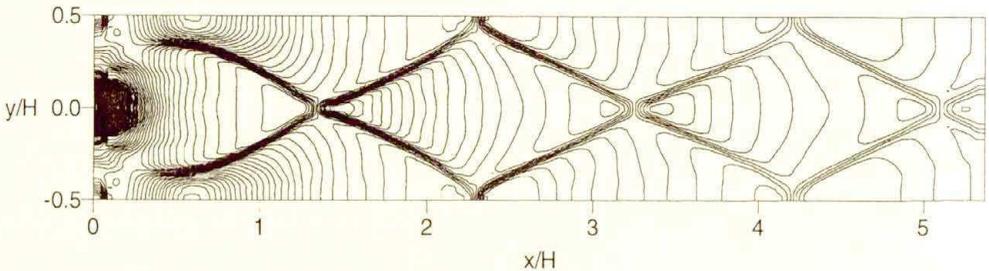


FIG. 3. Calculated steady-state solution (pressure contours).

Figure 4 shows the interferogram obtained from flow visualisation for identical conditions. Results of SZUMOWSKI and MEIER work [4] have been used.

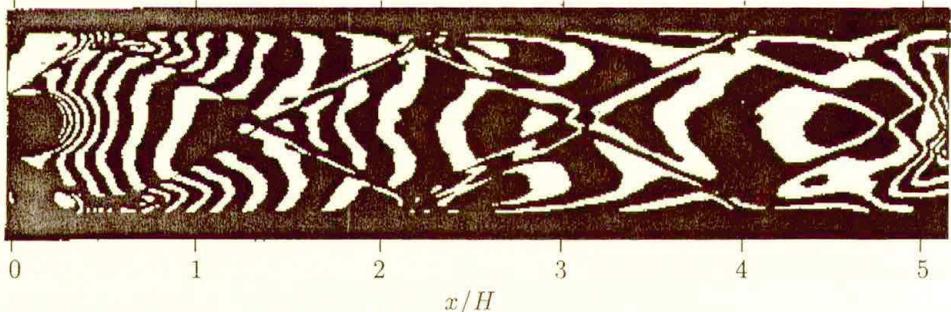


FIG. 4. Interferogram showing transonic channel flow.

As seen in Fig. 3 and Fig. 4, oblique shocks appearing in the flow are captured in the calculation accurately. The calculated structure of the flow agrees well with that observed in the real flow. The effect of a “double” wave seen in the interferogram, where the first shock is reflected from the wall, is a result of shock – boundary layer interaction. Hence, it cannot be obtained from the inviscid model. The first shock seen in the interferogram, is relatively strong and produces a small

separation “bubble”. The shock is reflected from the boundary of the separation area rather than from the wall.

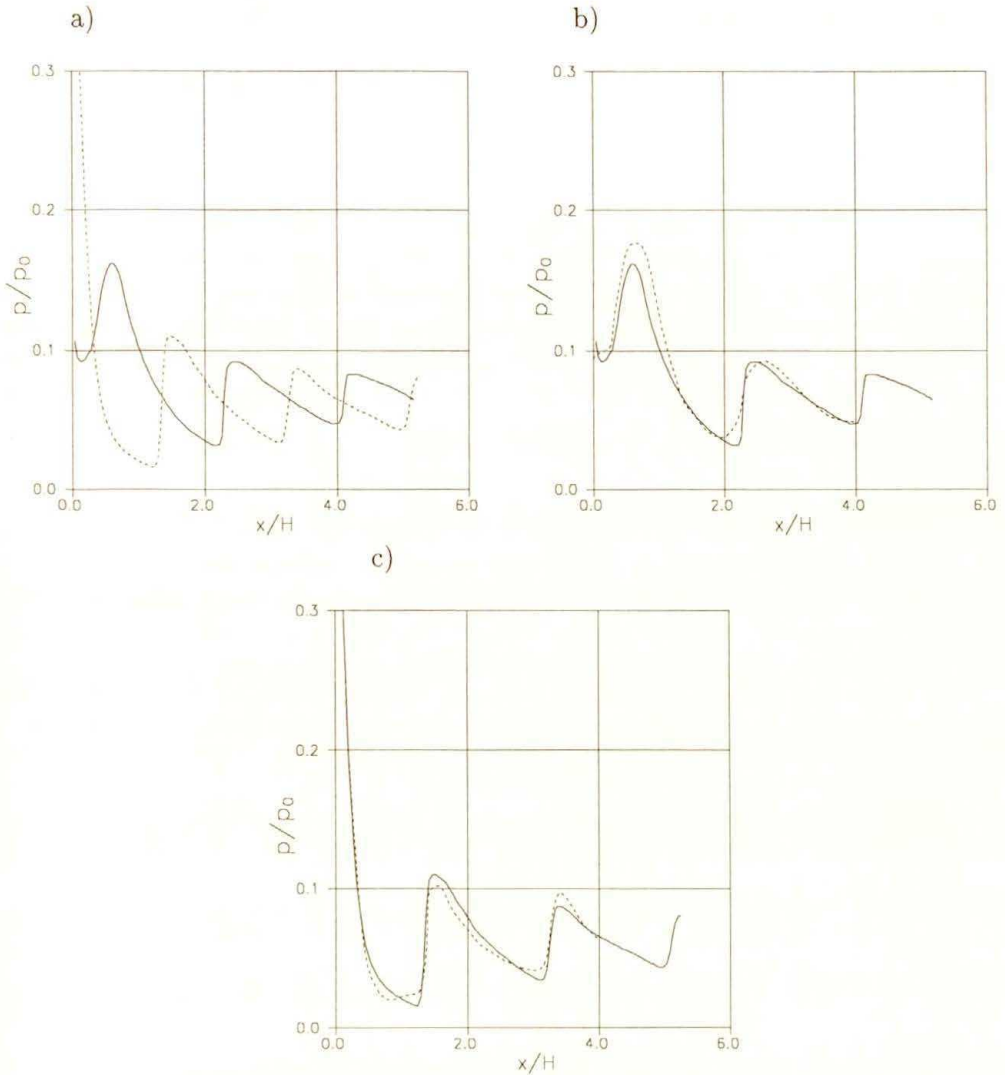


FIG. 5. a. Calculated pressure along the wall (solid line) and the axis (dashed line). b. Pressure along the channel wall: calculated (solid line) and measured (dashed line). c. Pressure along the channel axis: calculated (solid line) and measured (dashed line).

Figures 5 a, b, c show pressure distributions (non-dimensionalized with the inlet stagnation pressure) along the wall and the channel axis. Calculated values (Fig. 5 a) are compared with the measured ones for the wall (Fig. 5 b) and the axis (Fig. 5 c). Experimental data for the chosen case is provided by SZUMOWSKI and MEIER [4].

The calculated pressure distributions confirm the tendency of the shocks to become weaker along the channel. The decrease of shock amplitude is related to the increase of the entropy along the channel length. The largest differences between the calculated and measured pressures are seen for the wall distribution in the region where the supersonic stream hits the wall for the first time.

8. Conclusions

The presented numerical results are in good agreement with experiment. The calculated steady-state flow field properly reflects the presence and positions of oblique shocks occurring in the flow as well as their amplitudes. It is noticed that satisfactory results are obtained with relatively simple modelling of boundary conditions. It can be concluded that the selected numerical method based on two-step Lax – Wendroff algorithm can be effectively used for predicting transonic inviscid channel flows.

References

1. T. CHMIELNIAK, *Transonic flows* [in Polish], Ossolineum, Wrocław 1994.
2. C. HIRSH, *Numerical computation of internal and external flows*, Vol. 2, Wiley, N.Y. 1990.
3. R.D. RICHTMYER and K.W. MORTON, *Difference methods for initial value problems*, Wiley, N.Y. 1967.
4. A. SZUMOWSKI and G. MEIER, *Schwingungen der Überschallströmung in einem Kanal mit Querschnittssprung*, Rep. Max-Planck-Institut für Strömungsforschung, Göttingen 1978.

INSTITUTE OF AERONAUTICS AND APPLIED MECHANICS

WARSAW UNIVERSITY OF TECHNOLOGY.

e-mail: lis@meil.pw.edu.pl

Received February 7, 1997.
